Analytica Chimica Acta 673 (2010) 95–100

Contents lists available at ScienceDirect

Analytica Chimica Acta

journal homepage: www.elsevier.com/locate/aca

The effects of flow type on aptamer capture in differential mobility cytometry cell separations

Yan Liu [a], Se Won Bae [b,c], Kelong Wang [a], Jong-In Hong [b,c], Zhi Zhu [c], Weihong Tan [c], Dimitri Pappas [a,*]

[a] Department of Chemistry and Biochemistry, Texas Tech University, Lubbock, TX USA
[b] Department of Chemistry, Seoul National University, South Korea
[c] Center for Research at the Bio/Nano Interface, Department of Chemistry and Department of Physiology and Functional Genomics, Shands Cancer Center, UF Genetics Institute and McKnight Brain Institute, University of Florida, Gainesville, FL USA

ARTICLE INFO

Article history:
Received 10 March 2010
Received in revised form 11 May 2010
Accepted 12 May 2010
Available online 20 May 2010

Keywords:
Differential mobility cytometry
Aptamer
Cell separation
Cell capture time

ABSTRACT

In this work, differential mobility cytometry (DMC) was used to monitor cell separation based on aptamer recognition for target cells. In this device, open-tubular capillaries coated with Sgc8 aptamers were used as affinity chromatography columns for separation. After cells were injected into the columns, oscillating flow was generated to allow for long-term cell adhesion studies. This process was monitored by optical microscopy, and differential imaging was used to analyze the cells as they adhered to the affinity surface. We investigated the capture time, capture efficiency, purity of target and control cells, as well as the reusability of the affinity columns. Capture time for both CCRF-CEM cells and Jurkat T cells was 0.4 ± 0.2 s, which demonstrated the high separation affinity between aptamers and target cells. The capture efficiency for CCRF-CEM cells was 95% and purity was 99% in a cell mixture. With the advantage of both high cell capture efficiency and purity, DMC combined with aptamer-based separation emerges as a powerful tool for rare cell enrichment. In addition, aptamer-based DMC channels were found to be more robust than antibody based channels with respect to reuse of the separation device.

1. Introduction

Cell separations have played an important role in bioanalysis [1]. Applications as varied as CD4+ counting for AIDS patients [2–4], cancer cell detection/isolation [5–9], and bacterial detection [10–12] have been demonstrated in recent years, with the list of possible applications growing continuously. While many cell separation strategies exist, such as dielectrophoresis [13–15], palette arrays for adherent cell selection [16–17], selective lysis [18–19], and size-based sieving [20–21], cell affinity chromatography has remained a versatile technique for separating cells based on differences of cell-surface chemistry [22–27].

Recently, a new affinity separation method, differential mobility cytometry (DMC), was described [28–29]. DMC uses oscillating flow and differential imaging of a CCD camera to realize a new form of affinity capture and isolation. The benefits of DMC over other affinity methods include the use of the cell capture time to estimate the number of capture bonds formed and the ability to observe the same cells as they bind and interact with the surface. The DMC approach is based on preliminary work with open-tubular capillary separations [22], although any channel coated with affinity ligands can be used. The differential imaging approach allows for cells to be detected based on movement in the channel [30–32], and classified as free or bound. In addition, the difference in cell mobility can be used to observe surface interactions that result in incomplete cell capture, such as swaying or rolling on the affinity surface. Since differential imaging is used, cell capture can be performed rapidly without the use of labels, if desired.

The majority of cell affinity separations use antibodies or other protein-based capture molecules. The advantages of using antibodies—particularly monoclonal types—include high specificity (K_d in the pM–nM range for many antibody types), and wide availability. However, antibodies have distinct disadvantages, including the need for *a priori* knowledge of the antigen, pure samples of antigen for antibody production, and in some cases an inability to generate a functional antibody. Aptamers, DNA- or RNA-based capture ligands, address many of the disadvantages of antibodies and other capture proteins, and possess some unique advantages. Benefits of using aptamers include their smaller molecular weight, the ability to generate aptamers based on a wider variety of molecular targets, and the reproducibility of aptamer production once the nucleic acid sequence is known.

In recent years, a new approach to produce aptamers for cell capture has been introduced. This method, whole-cell SELEX (Systematic Evolution of Ligands by Exponential enrichment), uses positive enrichment of a target cell, followed by negative depletion by

* Corresponding author. Tel.: +1 806 742 3142.
E-mail address: d.pappas@ttu.edu (D. Pappas).

0003-2670/$ – see front matter © 2010 Elsevier B.V. All rights reserved.
doi:10.1016/j.aca.2010.05.017

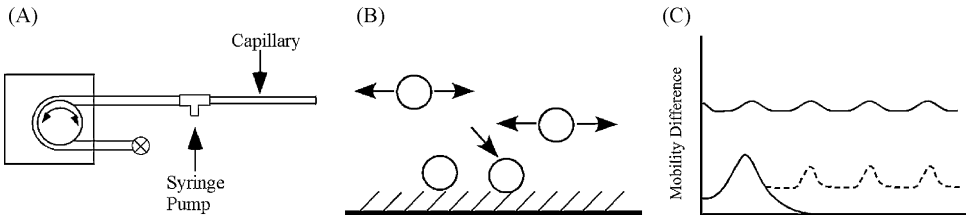

Fig. 1. (A) DMC system. (B) Captured cells and moving cells in the channel. (C) Mobility difference of adhered (lower trace, solid line), swaying (lower trace, dashed line), and rolling cells (upper trace).

a non-target cell [33]. The method is similar to SELEX used to generate aptamers for molecular targets, but knowledge of the surface markers of a cell is not needed. Aptamers generated by whole-cell SELEX have been used for selective capture of T cell leukemia cells [34], including measurements of cancer patient samples.

In this work, an aptamer sequence (Sgc8) generated using CCRF-CEM T leukemia cells was used as the capture ligand for differential mobility cytometry separations. The number of bonds formed during aptamer capture was determined, and the binding strength was characterized. Aptamer capture was found to be strong, as cells captured by the Sgc8 aptamer did not sway or roll on the surface, but adhered tightly upon capture. The effects of linear (unidirectional) and oscillating flow were also determined for DMC using the Sgc8 aptamer as the capture ligand. The robustness of the aptamer, combined with its high specificity for the target cell, allowed for DMC separations with higher separation affinity than previously reported [28]. Capture efficiency and purity, as well as testing using a non-leukemia T cell control, are presented.

2. Theory

Cell capture in any affinity separation is affected by cell-surface interactions. In affinity capture—regardless of the type of capture molecule used—the number of bonds formed during the capture process is the product of the cell-surface interaction area A_c, the antigen density of the cell B, and the time of the cell-surface interactions τ_c. According to Lauffenburger's formula [35], the cell will adhere if the shear force is less than the bond strength formed during the cell-surface interaction. The number of bonds is calculated as:

$$B^* = BA_c\tau_c$$

and the critical number of bonds needed to hold a cell to the affinity [1] surface is

$$B_c = \frac{F}{f_c}$$

Here, F is the shear force and f_c is the force of a single bond between the capture molecule and the cell. A stronger bond between the cell and capture molecule will result in a more rigidly held cell, or a cell that is captured with fewer bonds.

Using DMC, the number of bonds formed during a collision can be estimated. The cell-surface interaction area can be estimated by microscopy, and the antigen density can be measured by several methods [36], including flow cytometry and fluorescence correlation spectroscopy. The cell-interaction time is measured by DMC for each cell that is observed in the image frame. Using video acquisition (either white-light or fluorescence), cells are loaded under linear or oscillating flow and adhere to the capture surface. Differential imaging [28–29] is used to detect moving cells. The capture time is defined as the time between the peak mobility and when the cell stops moving on the affinity-surface. It is important to note that the capture time indicates the time required for the cell to come in contact with the surface and then stop (Fig. 1), but it does not include any additional movement such as the cell swaying on its anchor point. The additional movement is indicative of partial or weak capture, where the cell is held by enough affinity bonds to immobilize it on the surface, but not enough to completely stop all movement in the flowing stream (Fig. 1).

3. Experimental

3.1. DMC instrumentation

The DMC setup is similar to the one described in [28]. Briefly, an oscillation generator pump was used to produce push–pull flow in the capillary. A T-connector was used to connect the oscillation pump with the capillary (Fig. 1A). The capillary was made of fused silica, with 10 cm length and 200 μm inner diameter. The second port on the T-connector was used to inject sample into the capillary. The pulse speed and flow rate of the oscillating flow were controlled independently. The separation channel and pump were mounted on an inverted microscope (IX71, Olympus, Center Valley, PA, USA) using white-light imaging for most DMC measurements. For fluorescence imaging, a 100 W Hg lamp was used in conjunction with filter sets appropriate for the dyes used. For fluorescence imaging of mixtures, one cell type (either the target or control cell) was stained with CellTracker Green (Invitrogen).

The CCD camera (Orca, Hamamatsu, Bridgewater, NJ, USA) was operated in continuous-acquisition mode to generate video files. These raw files were used to generate DMC data. A frame difference (i.e. Frame t_1–Frame t_2) is produced to identify cell movement. The frame rate and the number of frames that elapse between the subtraction process dictate the temporal resolution. In this work, the time between frames was 0.67 s. Details of data analysis procedure are presented in [28–29].

3.2. Aptamer synthesis and biotinylation

The following aptamer has been selected for CCRF-CEM cells: sgc8, 5′-ATC TAA CTG CTG CGC CGC CGG GAA AAT ACT GTA CGG TTA GA-3′. The aptamer was synthesized on the ABI 3400 DNA/RNA synthesizer (Applied Biosystems, Foster City, CA, USA). Except for normal DNA bases, 5′-biotin group were also synthesized on machine. The synthesis protocol was set up according to the requirements specified by the reagents' manufacturers. After machine synthesis, the HPLC purification was performed with a cleaned Alltech C_{18} column (Econosil, 5 μm, 250 × 4.6 mm, Alltech, Deerfield, IL. USA) on a Prostar HPLC machine (Varian, Walnut Creek, CA, USA). The purified probe was quantified by determining the UV absorption at 260 nm with a Cary Bio-300 UV spectrometer (Varian), after which the probe was dissolved in DNA grade water and stored in the freezer at −20 °C for future experiments.

3.3. Conjugation approach

The conjugation strategy used in this work is based on previous cell affinity separations [22–23]. A layer of biotinylated bovine serum albumin (BSA) is deposited on the inner walls of the glass

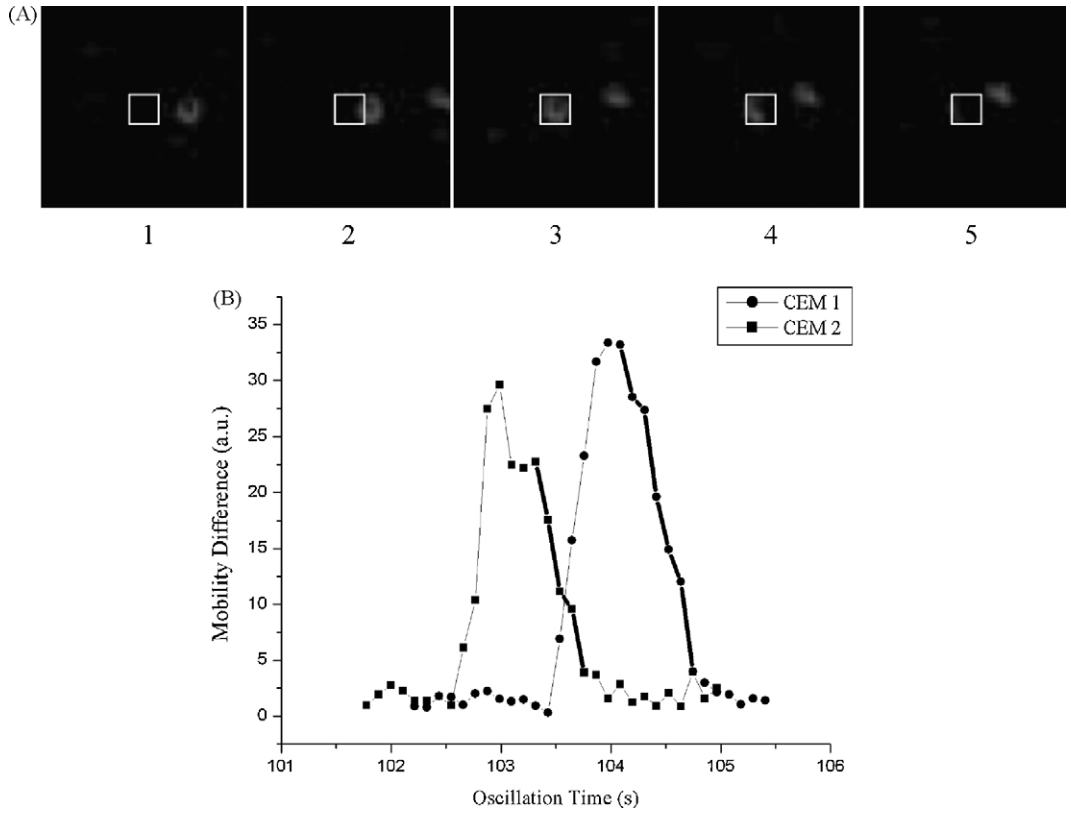

Fig. 2. (A) Mobility difference images of a cell entering the analysis window and adhering to the surface (the cell disappears as it adheres, since the mobility approaches zero). In (1–2) cells move into the window (motion is left-to-right). In (3) the cell is in the center of the window, indicated by the peak in the mobility difference curve (B). In (4–5), the cell stops moving and is anchored to the affinity-surface in the analysis window. The decrease in cell mobility is monitored as a decrease in differential image intensity. (B) Mobility difference measurements of two typical CCRF-CEM cells. Cells enter the window and the mobility difference increases, and then the cells adhere to the surface and the mobility difference decreases. a.u. (arbitrary units) is the difference in image intensity between two video frames.

channel. A layer of neutravidin is then introduced into the channel; the biotinylated Sgc8 aptamer is added in the final step, forming the affinity surface. The volume of regent loaded in the capillary is 3 μL per injection, as per methods detailed elsewhere [23].

3.4. Cells and cell culture

CCRF-CEM T cell leukemia, HuT 78 Cutaneous T cell, RPMI 8226 plasmacytoma cell, and Jurkat T cell lines were purchased from American Type Culture Collection. Each cell line was grown in RPMI 1640 medium supplemented with 10% fetal bovine serum and 20 mL L^{-1} penicillin–streptomycin solution (Sigma–Aldrich, St. Louis, MO, USA). Cells were maintained in an incubator at 37 °C and 5% CO_2 atmosphere before use. Cells were sub-cultured 1–2 times each week and typically 1–2 days before use. Cell densities varied between 10^5 and 10^6 cells mL^{-1} before use. Cells were centrifuged and washed with phosphate buffered saline (PBS, pH 7.4) containing 3% bovine serum albumin (BSA). This 3% BSA solution was used as the separation buffer as well. Separation occurred on the microscope stage without thermostatting or control of the atmosphere.

3.5. Separation system

Cells were loaded into the capillary using a syringe pump. Phosphate buffered saline containing 3% BSA was used as carrier fluid to minimize non-specific binding. After the capillaries were filled with cell suspension, either linear or oscillating flow was initiated. In linear flow, new cells were continuously introduced and suspended (unbound) cells were flushed out of the observation window. In oscillation, the residence time of the cells was longer. In this experiment, an optimized oscillation frequency of 20.7 pulses min^{-1} was used. For stop-flow measurements, cells were loaded into the capillary and allowed to settle to the surface for 10 min. Unbound cells were then flushed from the aptamer surface. Microscope images of the columns were taken before and after the washing steps to determine cell retention and removal efficiencies.

3.6. Cell detection

Cells were counted on-column using either transmission or fluorescence microscopy. Images were obtained at two positions along the channel. An objective (0.10NA, 4×) was used for white-light imaging and a 0.25NA, 10×objective was used for fluorescence imaging. Images were imported into ImageJ (v1.33, National Institute of Health, Bethesda, MD, USA) for analysis, while movie files were edited using Quicktime Pro (v.7.0, Apple Inc. Cupertino, CA, USA), compressed by VisualHub, and processed in the Image J.

Cell capture efficiency in oscillating flow was calculated by counting the number of cells attached on the capillary and unattached cells which kept moving in the capillary, respectively. The capture efficiency was calculated as:

$$E = \frac{n_{\mathrm{att}}}{n_{\mathrm{att}} + n_{\mathrm{unatt}}} \quad (1)$$

where n_{att} and n_{unatt} are the attached cells on the surface and unattached cells that moving in the capillary.

Cell retention efficiency in linear flow was calculated by measuring the number of cells before wash (after a 10 min settling time) and after wash. It is defined as:

$$E = \frac{n_{\mathrm{pre}} - n_{\mathrm{post}}}{n_{\mathrm{pre}}} \quad (2)$$

where n_{pre} and n_{post} are the cell counts before and after wash, respectively. The retention efficiency was calculated for each cell type.

3.7. Safety considerations

All cell lines are biosafety level 1 organisms. Cells were handled in a BSL 2A biosafety cabinet to preserve culture sterility. Personal protective equipment was worn at all times when handling cell samples.

4. Results and discussion

4.1. Aptamer capture time in column

The adhesion processes of CCRF-CEM (CEM), Jurkat T, HuT 78 T, and RPMI 8226 B cells using aptamer sequence (Sgc8) as capture ligands were analyzed by DMC. In oscillating flow, HuT 78 T and RPMI 8226 B cells remained mobile in the channels, while most of CEM and Jurkat T cells slowed down and attached on the aptamer-modified capillary surface. DMC has proven to be an effective method for obtaining accurate cell mobility information, including the adhesion time and cell sliding, swaying, rolling and so on.

Data analysis was processed by subtracting two CCD image streams [37]. These two image streams were derived from the same video file but had six-frame time difference (time interval 0.67 s). Fig. 2A shows difference images of a CEM cell (CEM 1 in Fig. 2B) at 103.4 s, 103.6 s, 104.0 s, 104.4 s, and 104.7 s. The intensity of these images represents the cell mobility difference. We fixed the analysis window on a specific region of the image, where the target cell would slow down and attach. The window size was approximately 100 μm^2, the same as cell the size, which can avoid other cells entering the window. From 103.4 s to 104.0 s, target cell moved into the analysis window, reflected in Fig. 2B as a sudden increase in the mobility difference value (brightness of the difference image). The cell reaches the center of the analysis window (the point of attachment) and begins to form affinity bonds and stops at 104.7 s. This is seen as both a decrease in mobility difference in Fig. 2B, and by the disappearance of the cell from the difference images in Fig. 2A (1–5). The mobility difference for this example cell (CEM 1) increased from 1 a.u. (1) to 33 a.u. (3) as it entered the window. The mobility difference then decreased to 3 a.u. (5) when the cell stopped completely. The mobility difference curve of a second example cell (CEM 2) featured a similar mobility curve as it entered its analysis window and was captured. Cell CEM 2 showed a slight shoulder on the decreasing side of the mobility difference time trace. This is attributed to the cell rolling on the surface after the initial interaction with the aptamers [28].

The adhesion time of cells can be calculated from the mobility difference. The adhesion time for each cell is from the point of cell-surface interaction to stopping completely (marked with broad lines in Fig. 2B). For cell CEM 1, the adhesion time was 0.7 s; the adhesion time for cell CEM 2 was 0.4 s. The mean adhesion time for all CEM cells measured was 0.37 ± 0.15 s (mean $\pm$ s.d.) ($n = 20$), and 0.38 ± 0.17 s ($n = 20$) for Jurkat T cells. Using Lauffenburger's model of cell adhesion, the capture time can be used to estimate the number of bonds formed in capture process [35]. From the similar adhesion time and similar cell sizes, we can conclude that this selected aptamer can be used for highly selective recognition of both CEM and Jurkat T cells.

The bond strength formed between aptamer and target cells is strong when compared with DMC work using antibodies as capture ligands. Adhesion time in aptamer capture is short. Most of cells stopped quickly after they attached on the surface. In antibody capture of similar cells, the cells attach to the surface but continue to rock or sway in the oscillating flow [28]. Only a few cells swayed on the aptamer-coated surface, indicating rigid capture and a high binding force.

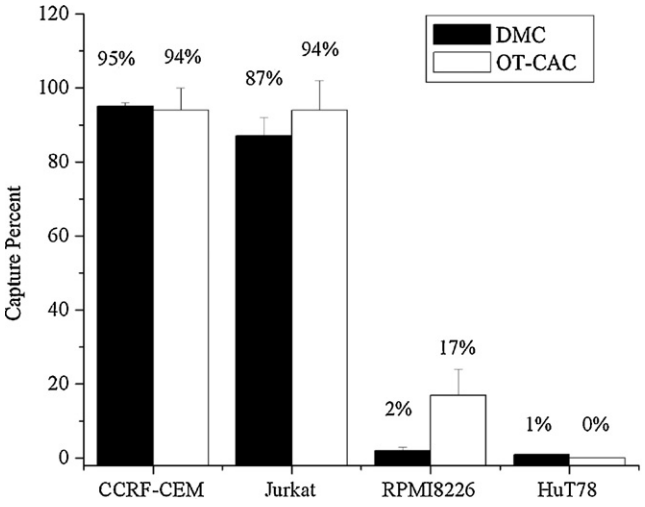

Fig. 3. Capture efficiency of CCRF-CEM, Jurkat T, RPMI 8226 B and HuT 78 T cells in oscillating (DMC) and linear flow (OT-CAC, (22)) channels. The non-specific binding is comparable for HuT 78 non-target cells, but 8.5 times worse for RPMI 8226 B non-target cells.

4.2. Comparison of linear flow and oscillating DMC flow using aptamers

Since the Sgc8 aptamer has high selectivity for CEM target cells [38], we used DMC to investigate the capture efficiency of aptamer-coated capillaries for target as well as other cell types. To clearly show the selectivity of aptamer-coated capillary, four cell lines: CEM, Jurkat T, HuT 78 T, and RPMI 8226 B cells were separated using DMC in both linear and oscillating flow, respectively. The capture efficiencies of CEM, Jurkat T, HuT 78 T, and RPMI 8226 B cells in DMC and linear flow are shown in Fig. 3. The Sgc8 aptamer has high selectivity to CEM and Jurkat T cells with capture efficiencies of 95% and 87% in oscillating, and 94% and 94% in linear flow (CEM and Jurkat, respectively). The capture efficiency in oscillating flow for RPMI 8226 and HuT 78 cells was 2% and 1%, respectively. There was no non-specific binding of HuT 78 cells in linear flow (i.e. zero HuT 78 cells were captured), but the non-specific capture of RPMI 8226 cells was 17%. All experiments were performed in triplicate, and the reported error is the standard deviation. Comparing the results of the two flow approaches systems, oscillating flow has lower overall non-specific binding and provides adhesion information that linear flow cannot. This is because non-specific binding usually increases as flow rate decreases [38]. In linear flow, the flow profile is laminar and the minimal shear force is at the channel surface. In oscillating flow, the flow is not laminar and we anticipate that shear force is greater at the channel surface for a given volumetric flow rate. However, both flow modes should be evaluated in individual cases to ensure optimum performance.

Because of the limits in the depth of field of the imaging system (8 μm for a 10$\times$ objective), only cells located on the bottom portion of the capillary wall were detected. The cell numbers obtained from the images were less than the total numbers in the capillary, even though most of cells settled to the surface via sedimentation. In future work, microchannels with lower ceilings will be used in order to avoid this issue. When continuous flow was applied to the cell separation, high separation purity of target cells was obtained, but the capture efficiency was much lower than in oscillating flow

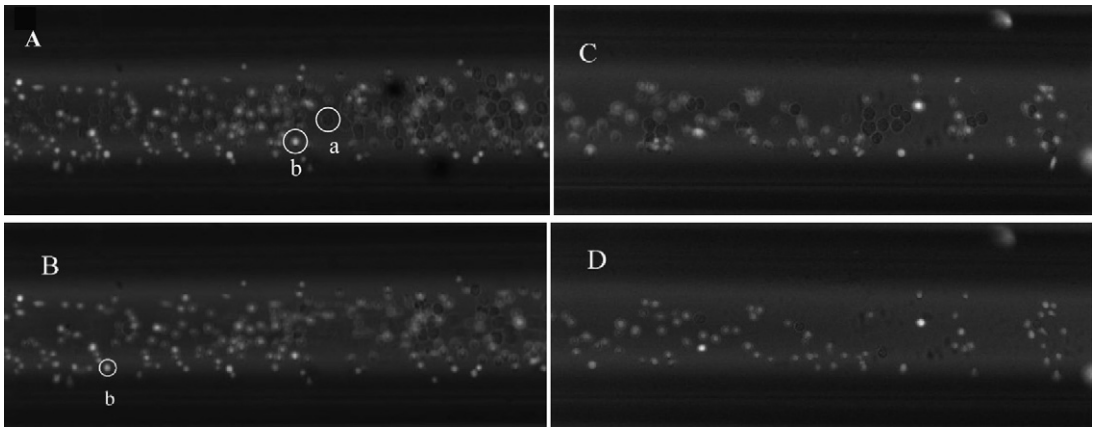

Fig. 4. Selective binding of aptamer to target cells in DMC and OT-CAC using fluorescence microscopy. (A) Image of mixed cells in the capillary at oscillation time of 2 min. A HuT 78 non-target cell is dark and marked as a; a CCRF-CEM target cell is white one and marked as b. (B) Average of six images, in which cells captured on the aptamer-coated surface can be identified. (C) Image of mixed cells captured on the aptamer-coated surface before wash with buffer in a linear flow OT-CAC channel. (D) The OT-CAC channel after wash with buffer at 2.0 mL h^{-1}.

as cells may leave the channel before interacting with the surface [38].

4.3. Mixture analysis

To demonstrate the selection potential of DMC using aptamer-immobilized channels, a mixture of target and control cells was passed through the flow cell in order to separate the cells according to the binding affinity. A 2:1 ratio of CEM and HuT 78 T cells was used. HuT 78 cells have a cell radius that is 1.6 times larger than CEM cells. The HuT 78 cells therefore have a larger cell-surface contact area, increasing the probability of non-specific binding. In order to distinguish the cells in the DMC channels, CEM cells were incubated with CellTracker Green, and both transmission and fluorescence microscopy were employed to visualize the cells. As expected, the Sgc8 aptamer retained most of the CEM cells, while most HuT78 T cells remained free (Fig. 4). The purity of CEM cells was 99% in oscillating flow, and 94% in linear flow.

The fluorescence image of a cell mixture in a DMC channel at 2 min is shown in Fig. 4A. The bright cell (labeled b) is a CEM cell, and dark cell (labeled a) is a HuT 78 T cell, which is not as distinct as the dyed cells but can be seen clearly in white-light images (not shown). Fig. 4B is the average projection of six frames of the mixture at 2 min using Image J software. In this picture, only attached cells can be identified, because cells that moved quickly appeared blurred due to the relatively long exposure time. From those two pictures, we can find that most cells attached to the surface are CEM cells. The dynamic states of these cells were further confirmed by comparing fluorescent images to videos. We found that not all the HuT 78 T cells in Fig. 4B were attached. Some of them were wagging at that time, and were removed at higher flow velocity. As before, attached cells were counted after oscillating flow for 10 min. Of all the 197 attached cells, only two cells were HuT 78 T cells in this test. Fig. 4C and D shows the retention of target cells when linear flow was used in another channel. Most of the HuT 78 control cells were washed away at wash speed of 2.0 mL h^{-1}. Although the purity reached 94% using linear flow, non-specific binding remains problematic for the rarest cell concentrations.

4.4. Reuse of DMC columns

Aptamers are more robust than many of their antibody analogs, and can be subjected to suboptimum conditions for longer periods of time. Therefore, the reusability of aptamer-coated columns was investigated. In previous work [1,37], antibody-coated cell separation devices could be used only once. The inability to reuse columns is presumably due to elution conditions that rendered the antibodies non-functional after separation. The same elution conditions were used with aptamer-coated channels to directly compare the robustness of aptamers for DMC separations. In this test, cells were loaded into a PDMS-glass DMC channel. After capture, cells were then washed with 3% BSA buffer at a flow rate of 2.0 mL h^{-1}, which was sufficient to remove unbound cells. The retention efficiencies of five successive separations (spanning 8 h) were 94%, 94%, 96%, 92%, and 91%, respectively. The higher retention efficiency in the third test when compared with the first and second test was due to intra-system variation and was comparable to the variation for other cell capture systems [22]. More than 90% retention efficiencies in all these five tests are sufficient to illustrate that the stability of aptamer-coated DMC channels were superior to DMC devices using antibodies. In addition, it is possible to conserve reagents and devices by reusing them in some cases. The inter-day longevity of DMC channels using aptamers will be studied in future work.

5. Conclusion

Differential mobility cytometry was demonstrated using an aptamer as the capture ligand. The improved stability of the aptamer over traditional antibodies enhanced the performance of DMC separations. The Sgc8 aptamer used in this work was able to capture target cells with high selectivity and low non-specific binding. The short adhesion time (measured by DMC) corresponds to a strong affinity bond between the cell and the aptamer surface. In addition, cells attaching to the aptamer surface adhered tightly (no swaying), as compared to antibody surfaces which typically display cell movement around the cell-surface anchor point. In future work, we will study the effect of aptamer surface density on cell adhesion.

Compared with other separation systems, the aptamer-based DMC system has several advantages in capture efficiency and purity. The oscillation system can retain cells in the separation channel, effectively increasing the separation column indefinitely. In oscillating flow, cells have adequate time to interact with the affinity surface, which improved the efficiency of target cells when compared to linear flow systems. However, non-specific binding must be evaluated in both oscillating and linear flow, and the best flow mode chosen for the experiment at hand.

Differential imaging was used to obtain accurate cell mobility information. Compared with a test antibody, the aptamer shows higher capture affinity to target cells. The adhesion time of target

cells was 0.37–0.38 s. Based on Lauffenburger's formula [35], the adhesion time, the number of aptamer per unit area on the cell-surface [39], and the collision area between the cell and the surface, the number of bonds formed can be estimated. For CCRF-CEM cells, the density of aptamer is estimated to be 14,000 aptamers μm^{-2} based on Reif's estimation [37], capture time is 0.37 ± 0.15 s, and collision area can be estimated to be $2\,\mu m^2$ [28], consequently approximately 500–1500 bonds were formed during DMC capture using oscillating flow. The large range arises from the random nature of cell-surface interactions, not from DMC systems or other measurements.

DMC can be used for a variety of cell analysis applications, including the study of cell adhesion, detachment, and the change in ligand density over time. Aptamers have enhanced the performance of DMC, and as new aptamers are generated for cell targets, new DMC approaches can be developed with high specificity and capture efficiency.

Acknowledgements

D.P. was supported in part by a grant from the Robert A. Welch Foundation (Grant D-1667).

References

[1] D. Pappas, K. Wang, Anal. Chim. Acta 601 (2007) 26–35.
[2] X. Cheng, D. Irimia, M. Dixon, K. Sekine, U. Demirci, L. Zamir, R.G. Tompkins, R. Rodriguez, M. Toner, Lab Chip 7 (2007) 170–178.
[3] X. Cheng, D. Irimia, M. Dixon, J. Ziperstein, U. Demirci, L. Zamir, R.G. Tompkins, M. Toner, R. Rodriguez, J. Acquir. Immune. Defic. Syndr. 45 (2007) 257–261.
[4] K. Sekine, A. Revzin, R.G. Tompkins, M. Toner, J. Immunol. Methods 313 (2006) 96–109.
[5] X. Chen, Y. Huang, W. Tang, J. Biomed. Nanotechnol. 4 (2008) 400–409.
[6] J.E. Smith, C.D. Medley, Z. Tang, D. Shangguan, C. Lofton, W. Tan, Anal. Chem. 79 (2006) 3075–3082.
[7] J.K. Herr, J.E. Smith, C.D. Medley, D. Shangguan, W. Tan, Anal. Chem. 78 (2006) 2918–2924.
[8] H. Chen, C.D. Medley, K. Sefah, D. Shangguan, Z. Tang, L. Meng, J.E. Smith, W. Tan, ChemMedChem 6 (2008) 991–1001.
[9] J.C. Norton, L.S. Gollohan, S.E. Holt, W.E. Wright, J.W. Shay, Proc. Am. Assoc. Cancer Res. Annu. Meeting (1997) 504.
[10] J.B. Delehanty, F.S. Ligler, Anal. Chem. 74 (2002) 5681–5687.
[11] A.W. Lantzz, Y. Bao, D.W. Armstrong, Anal. Chem. 79 (2007) 1720–1724.
[12] M.A. Rodriguez, A.W. Lantz, D.W. Armstrong, Anal. Chem. 78 (2006) 4759–4767.
[13] X. Hu, P.H. Bessette, J. Qian, C.D. Meinhart, P.S. Daugherty, H.T. Soh, PNAS 102 (2005) 15757–15761.
[14] M. Hashimoto, H. Kaji, M. Nishizawa, Biosens. Bioelectron. 24 (2009) 2892–2897.
[15] M.D. Vahey, J. Voldman, Anal. Chem. 80 (2008) 3135–3143.
[16] H. Shadpour, C.E. Sims, R.J. Thresher, N.L. Allbritton, Cytometry Part A 75A (2009) 121–129.
[17] G.T. Salazar, Y. Wang, G. Young, M. Bachman, C.E. Sims, G. Li, N.L. Allbritton, Anal. Chem. 79 (2007) 682–687.
[18] P. Sethu, M. Anahtar, L. Moldawer, R. Tompkins, M. Toner, Anal. Chem. 76 (2004) 6247–6253.
[19] D. Irimia, R. Tompkins, M. Toner, Anal. Chem. 76 (2004) 6137–6143.
[20] S. Yang, S. Hsiung, Y. Hung, C. Chang, T. Liao, G. Lee, Meas. Sci. Technol. 17 (2006) 2001–2009.
[21] L. Wang, L.A. Flanagan, N.L. Jeon, E. Monuki, A.P. Lee, Lab Chip 7 (2007) 1114–1120.
[22] K. Wang, B. Cometti, D. Pappas, Anal. Chim. Acta 601 (2007) 1–9.
[23] K. Wang, M.K. Marshall, G. Garza, D. Pappas, Anal. Chem. 80 (2008) 2118–2124.
[24] M.B. Dainiak, F.M. Plieva, I.Y. Galaev, R. Hatti-Kaul, B. Mattiasson, J. Biotechnol. Prog. 21 (2005) 644–649.
[25] A. Kumar, A. Rodriguez-Caballero, F.M. Plieva, I.Y. Galaev, K.S. Nandakumar, M. Kamihira, R. Holmdahl, A. Orfao, B. Mattiasson, J. Mol. Recognit. 18 (2005) 84–93.
[26] M.B. Dainiak, I.Y. Galaev, B. Mattiasson, J. Chromatogr. A 1123 (2006) 145–150.
[27] A. Higuchi, A. Iizuka, Y. Gomei, T. Miyazaki, M. Sakurai, Y. Matsuoka, S.H. Natori, J. Biomed. Mater. Res. 78A (2006) 491–499.
[28] K. Wang, K. Solis-Wever, C. Aguas, Y. Liu, P. Li, D. Pappas, Anal. Chem. 81 (2009) 3334–3343.
[29] R.D. Reif, K. Wang, D. Pappas, Anal. Bioanal. Chem. 395 (2009) 2411–2413.
[30] J.M. Meinders, H.C. Van der Mei, H.J. Busscher, J. Microbiol. Methods 16 (1992) 119–124.
[31] H.J. Busscher, H.C. Van der Mei, Clin. Microbiol. Rev. 19 (2006) 127–141.
[32] P.K. Sharma, M.J. Gibcus, H.C. Van der Mei, H.J. Busscher, Appl. Environ. Microbiol. 71 (2005) 3668–3673.
[33] D. Shangguan, Y. Li, Z. Tang, Z.C. Cao, H.W. Chen, P. Mallikaratchy, K. Sefah, C.J. Yang, W. Tan, Proc. Natl. Acad. Sci. USA (2006) 11838–11843.
[34] J.A. Phillips, D. Lopez-Colon, Z. Zhu, Y. Xu, W. Tan, Anal. Chim. Acta 621 (2008) 101–108.
[35] C.M. Hertz, D.J. Graves, D.A. Lauffenburger, Biotechnol. Bioeng. 27 (1985) 603–612.
[36] D. Pappas, Practical Cell Analysis, John Wiley and Sons, 2010, pp. 279-281.
[37] R.D. Reif, K. Wang, D. Pappas, Anal. Bioanal. Chem. 295 (2009) 787–795.
[38] J.A. Philips, Y. Xu, Z. Xia, Z. Fan, W. Tan, Anal. Chem. 81 (2009) 1033–1039.
[39] Y. Chen, A. Munteanu, Y.F. Huang, J. Phillips, Z. Zhu, M. Mavros, W. Tan, Chem. Eur. J. (2009) 5327–5336.